

ORIGINAL ARTICLE

Open Access



Comparison of four different screw configurations for the fixation of Fulkerson osteotomy: a finite element analysis

Faruk Aykanat¹ , Ozkan Kose^{2*} , Bulent Guneri³ , H. Kursat Celik⁴ , Albert Cakar⁵ , Ersin Tasatan⁶  and Mihaela-Elena Ulmeanu⁷ 

Abstract

Background Conventionally, two 4.5 mm cortical screws inserted toward the posterior tibial cortex are usually advocated for the fixation of Fulkerson osteotomy. This finite element analysis aimed to compare the biomechanical behavior of four different screw configurations to fix the Fulkerson osteotomy.

Materials and methods Fulkerson osteotomy was modeled using computerized tomography (CT) data of a patient with patellofemoral instability and fixed with four different screw configurations using two 4.5 mm cortical screws in the axial plane. The configurations were as follows: (1) two screws perpendicular to the osteotomy plane, (2) two screws perpendicular to the posterior cortex of the tibia, (3) the upper screw perpendicular to the osteotomy plane, but the lower screw is perpendicular to the posterior cortex of the tibia, and (4) the reverse position of the screw configuration in the third scenario. Gap formation, sliding, displacement, frictional stress, and deformation of the components were calculated and reported.

Results The osteotomy fragment moved superiorly after loading the models with 1654 N patellar tendon traction force. Since the proximal cut is sloped (bevel-cut osteotomy), the osteotomy fragment slid and rested on the upper tibial surface. Afterward, the upper surface of the osteotomy fragment acted as a fulcrum, and the distal part of the fragment began to separate from the tibia while the screws resisted the displacement. The resultant total displacement was 0.319 mm, 0.307 mm, 0.333 mm, and 0.245 mm from the first scenario to the fourth scenario, respectively. The minimum displacement was detected in the fourth scenario (upper screw perpendicular to the osteotomy plane and lower screw perpendicular to the posterior tibial cortex). Maximum frictional stress and maximum pressure between components on both surfaces were highest in the first scenario (both screws perpendicular to the osteotomy plane).

Conclusions A divergent screw configuration in which the upper screw is inserted perpendicular to the osteotomy plane and the lower screw is inserted perpendicular to the posterior tibial cortex might be a better option for the fixation of Fulkerson osteotomy.

Level of evidence Level V, mechanism-based reasoning.

Keywords Finite element analysis, Tibial tubercle osteotomy, Fulkerson osteotomy, Screw fixation, Biomechanics

*Correspondence:

Ozkan Kose
drozkankose@hotmail.com

Full list of author information is available at the end of the article



© The Author(s) 2023. **Open Access** This article is licensed under a Creative Commons Attribution 4.0 International License, which permits use, sharing, adaptation, distribution and reproduction in any medium or format, as long as you give appropriate credit to the original author(s) and the source, provide a link to the Creative Commons licence, and indicate if changes were made. The images or other third party material in this article are included in the article's Creative Commons licence, unless indicated otherwise in a credit line to the material. If material is not included in the article's Creative Commons licence and your intended use is not permitted by statutory regulation or exceeds the permitted use, you will need to obtain permission directly from the copyright holder. To view a copy of this licence, visit <http://creativecommons.org/licenses/by/4.0/>.

Introduction

Tibial tubercle (TT) anteromedialization osteotomy, also called Fulkerson osteotomy, has become a standard surgical procedure in patients with patellofemoral (PF) instability associated with increased TT lateralization [1, 2]. This procedure effectively decreases the tibial tubercle–trochlear groove (TT–TG) distance and corrects the excessive Q angle [2, 3]. Secondly, it provides TT anteriorization that reduces the PF contact pressures [2]. Many previous studies have reported that Fulkerson osteotomy is a safe and effective procedure; however, it is not without complications [1–5]. Nonunion or delayed union, tibial fracture at the distal edge of the osteotomy, loss of knee range of motion, skin irritation due to prominent hardware, superficial and deep infection, failure of fixation, and neurovascular injuries have all been reported [2–5].

Proper planning and performance of the osteotomy, secure fixation, and maintaining the stable fixation until the bony union is crucial to prevent implant failure and complications [3, 5]. The fixation should be stable enough for early weight-bearing and active rehabilitation to preserve knee movements and thigh muscle mass. Conventionally, two parallel 4.5 mm cortical screws inserted toward the posterior tibial cortex are usually advocated for the fixation of the Fulkerson osteotomy [6]. However, the screws inserted by this method may not provide sufficient stability since the osteotomy plane is oblique. According to the AO principles, screws placed perpendicular to the fracture or osteotomy plane provide optimal compression and reduction [7]. Furthermore, bicortical fixation is well known to be stronger than unicortical fixation [7]. But, the penetration of the posterior cortex might cause iatrogenic neurovascular injuries because the popliteal nerve and artery lie posterior to the posterior tibial cortex [8, 9]. Finally, the screw heads may remain prominent when inserted perpendicular to the posterior cortex. On the other hand, screws inserted perpendicular to the osteotomy plane might be advantageous since they move away from the direct contact area during kneeling and are covered by the muscle mass (Fig. 1).

John Fulkerson first described anteromedialization tibial tubercle osteotomy in 1983 [10]. In his original technical description, it was reported that osteotomy fixation could be done via bicortical fixation with a single cortical lag screw or unicortical with a single cancellous lag screw without penetration of the posterior tibial cortex to avoid neurovascular structures. Since then, a limited amount of biomechanical research on how to fix a tibial tubercle osteotomy has been performed in the current literature (Table 1) [6, 11–19]. Screws of various thicknesses (3.5, 4.0, 4.5 mm),

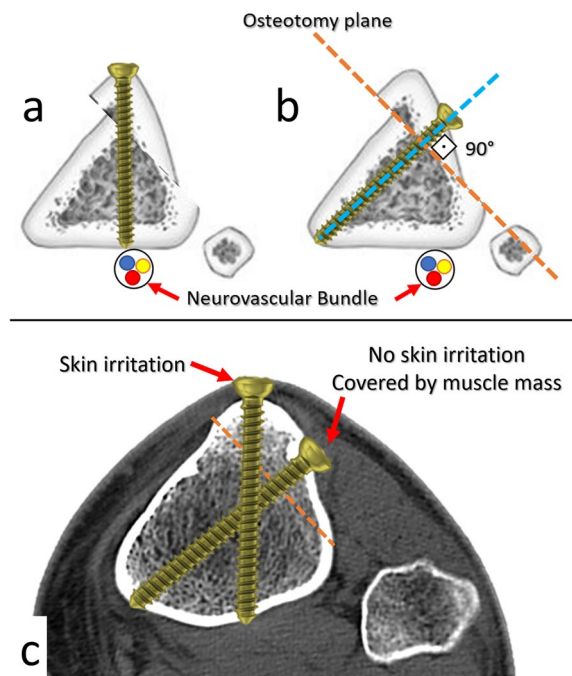


Fig. 1 Illustration showing the insertion of screw perpendicular to the posterior tibial cortex (a), and perpendicular to the osteotomy plane (b). Please note the risk of neurovascular injury with the first configuration. A screw inserted perpendicular to the osteotomy plane is covered by the muscle mass (c)

numbers (two or three), designs (fully threaded or partially threaded), materials (stainless steel, titanium, and bioabsorbable polymers), cerclage applications, plate fixation, and augmentation techniques have been reported. The screws used in almost all of these studies were placed in the anterior–posterior direction, as recommended by the original description of the technique. Only three studies examine the effect of different screw configurations on the fixation stability of tibial tubercle osteotomies. Chang et al. evaluated the gap formation, contact pressure, and stress distribution on the osteotomy plane created by six different combinations by changing the configurations of the screws in the sagittal plane. In the other study, Fulkerson osteotomy with distalization was modeled, and the screws were inserted toward the posteromedial cortex in the axial plane. However, no previous study examined the effect of axial plane divergence of screws in the axial plane on the stability of standard Fulkerson osteotomy.

Our study hypothesized that stability would increase if the screws were placed perpendicular to the osteotomy plane. Stable fixation is essential for the early initiation of rehabilitation and weight-bearing after the osteotomy, as well as the prevention of complications.

Table 1 Previous biomechanical studies on the biomechanical behavior of the various fixation methods of tibial tubercle osteotomy

Author	Year	Type of study	Model	Fixation methods	Results
Cosgarea et al.	1999	Cadaver (13 pairs)	Fulkerson osteotomy flat osteotomy	Two 3.5 mm screws (screw material unspecified)	The flat osteotomy resulted in a higher load to failure compared with Fulkerson osteotomy (1639 N versus 1166 N, $P < 0.05$)
Davis et al.	2000	Cadaver (36 unpaired knees)	Bevel-cut and step-cut flat osteotomies	Two 4.5 mm cortical screws versus 18-gauge stainless (either three- or four-level) cerclage	The failure load for the bevel-cut osteotomies repaired with two screws was 1654 ± 359 N; for the bevel-cut osteotomies repaired with three cerclage wires, 622 ± 283 N; for the step-cut osteotomies repaired with three cerclage wires, 984 ± 441 N; and for the step-cut osteotomy repaired with four cerclage wires, 1099 ± 632 N
Caldwell et al.	2004	Cadaver (40 unpaired tibia)	Flat osteotomy	Two 4.5 mm bicortical screws 18-gauge stainless four-level cerclage. Traction force at 0° and 25°	Screw constructs failed at 1429 ± 348 N (0°) and at 1925 ± 982 N (25°). Wire constructs failed at 1072 ± 260 N (0°) and at 893 ± 293 N (25°)
Warner et al.	2013	Cadaver (5 pairs)	Fulkerson osteotomy	Two 4.5 mm screws versus Three 3.5 mm screws	The maximum failure load for osteotomies secured with two 4.5-mm screws was 1459 ± 540 N, and for three 3.5-mm screws, it was 1360 ± 707 N ($P = 0.723$)
Nurmi et al.	2017	Cadaver (22 pairs)	Flat osteotomy (straight cut)	4.5-mm PLLA screws versus 4.5 mm stainless steel screws	The mean yield load was 566 ± 234 N in the bioabsorbable screw group and 984 ± 630 N in the metal screw group ($P = 0.002$)
Chang et al.	2019	FEA	Flat osteotomy	Two titanium 4.5 mm screws with six configurations: parallel horizontal screws placed at a 20 mm interval, parallel horizontal screws placed at a 30 mm interval, parallel upward screws, parallel downward screws, trapezoid screws, and divergent screws	The configuration of two parallel downward screws yielded the highest stability with the lowest fragment displacement and gap opening. The configuration of two upward screws resulted in the highest fragment displacement and gap deformation between the fragment and tibia. The stress of the osteotomized bone fragment was highest with the configuration of two upward screws
Chang et al.	2019	FEA	Flat osteotomy with three fragment shapes: step cut, bevel cut, and straight cut	Two titanium 4.5 mm screws with three configurations: parallel horizontal screws with an interval of 20 mm, trapezoidal screws with an angle of 45° , and parallel downward screws with an interval of 15 mm	The step cut resulted in higher stability than the bevel and straight cut, but the stress was higher. Among the screw configurations, two parallel downward screws resulted in the highest stability, given the same fragment shape. In the horizontal configuration, the step-cut tibia developed the largest contact force to achieve stability of the bone fragment under loading
Chen et al.	2019	FEA	Flat osteotomy (step cut) with 1 mm gap formation either in proximal or distal contact surfaces	Two titanium 4.5 mm screws with six configurations: parallel horizontal screws placed at a 20 mm interval, parallel horizontal screws placed at a 30 mm interval, parallel upward screws, parallel downward screws, trapezoid screws, and divergent screws	Proximal gap model resulted inferior results compared with distal gap model in all screw configurations. Among the screw configurations, two parallel downward screws resulted in the highest stability in both models

Table 1 (continued)

Author	Year	Type of study	Model	Fixation methods	Results
Gunerı et al.	2021	FEA	Fulkerson osteotomy + distalization	Two 3.5 mm cortical screws, Two 4.5 mm cortical screws Three 3.5 mm cortical screws Three 4.5 mm cortical screws Three 3.5 mm screws with 1/3 tubular plate Four 3.5 mm screws with 1/3 tubular plate	Maximum sliding (0.660 mm), gap formation (0.661 mm), and displacement (1.267 mm) were seen with two 3.5 mm screw fixation, followed by two 4.5 mm screws, three 3.5 mm screws, and three 4.5 mm screws, respectively, in the screw group. The minimum displacement was observed with a plate, and two 3.5 mm screw fixation models
Frame et al.	2021	Cadaver (5 pairs)	Flat osteotomy	Two parallel 4.0 mm partially threaded cannulated screws versus Two parallel 4.0-mm partially threaded cannulated screws plus a nonabsorbable suture tape (FiberTape) in a figure-of-8 construct	Two specimens of the standard group exhibited clinical failure during cyclic loading to 400 N. All other specimens survived cyclic loading to 800 N. The mean ultimate failure load after the pull-to-failure test was 2475 ± 554 N for the augmented group and 1475 ± 280 N for the standard group
Current study	2022	FEA	Fulkerson osteotomy	Two 4.5 mm cortical screws were tested in four different configurations (1) Both screws are perpendicular to the osteotomy plane (2) Upper screw is perpendicular to the tibial cortex; the lower screw is perpendicular to the osteotomy plane (3) Both screws are perpendicular to the posterior tibial cortex (4) Upper screw is perpendicular to the osteotomy plane; the lower screw is perpendicular to the posterior tibial cortex	The minimum total displacement was observed in the fourth scenario, which resulted in the highest stiffness

Materials and methods

Study design and finite element method

This study utilized finite element methods that were carried out under static loading conditions and homogeneous isotropic linear elastic model assumptions. Besides, nonlinear contact behavior between related components was considered. Fulkerson osteotomy was generated, and the model was fixed with four different screw configurations.

FEA is a numerical method that utilizes models and simulations to examine the mechanical behavior of an object under certain physical conditions in a virtual computer environment. In the finite element method, complex 3D geometric objects are divided into small elements connected with nodes; this procedure is also called spatial discretization. Models can be created using computerized tomography data to simulate real bony geometry. Material properties, contact definitions, and boundary conditions are defined and entered into the software. Finally, force–displacement equations of each small element can easily be computed and combined for the entire structure. Thus, displacements, including sliding and gapping, and strains and stresses arising from these displacements, can be calculated and visualized throughout the model and its components.

Currently, the gold standard for assessing the initial stability of fracture or osteotomy fixation remains biomechanical testing using cadaveric models. However, FEA has several advantages over conventional biomechanical experiments. First, this method is cheaper than using fresh cadavers. Second, a complete inspection of the model throughout the entire structure is possible. Conversely, assessing internal strain and damage is exceptionally challenging in cadaver models.

Additionally, it is unaffected by geometric variations and bone quality differences between cadavers, which is a significant confounding factor. Another advantage of FEA simulations over biomechanical testing is the ability to evaluate and compare alternative implant designs or configurations of the same implant within the same bone. Moreover, new implant designs might be tested and modified without manufacturing the final prototype. Besides these advantages, FEA inherits certain disadvantages. Simplifying complex geometry and using predefined assumptions regarding material properties and boundary conditions are the significant limitations of the technique. Secondly, the divergence of the models from clinical reality, model verification, and validation are other significant obstacles that might result in misleading interpretations. Since FEA is fundamentally a metamathematical method that finds approximated solutions to biomechanical problems, errors in FEA are inevitable. Thus above-mentioned

pros and cons should be considered when evaluating the outputs [20–22].

Modeling of the Fulkerson osteotomy

Computerized tomography (CT) data of a 20-year-old male patient (height 174 cm and weight 76 kg) with recurrent patellar dislocation was used to create the tibial model. The tibial tubercle–trochlear groove (TT–TG) distance was abnormal (23 mm), and Fulkerson osteotomy was indicated for the patient. A TT–TG distance larger than 20 mm is accepted as abnormal.

The CT imaging was performed using the CT scanner (Siemens go.Up, Siemens, Munich, Germany) installed in the authors' university hospital. The following were the scan parameters: a total of 232 axial slices were taken at 120 kV, 30 mA, slice distance of 1.0 mm, FoV: 218 mm, from the supracondylar femur to the proximal tibia. The patient gave written informed agreement to the anonymous use of the imaging files. To model and simulate the FEA scenarios, Materialise Mimics–Medical 3D image-based engineering software (Materialise NV, Belgium), SolidWorks parametric solid modeling software (Dassault Systems SolidWorks Corp, Waltham, USA), and ANSYS Workbench FEA code (ANSYS, Ltd., Canonsburg, PA, USA) were used.

The Fulkerson osteotomy was modeled following prior descriptions [10]. The osteotomy length was 72 mm, and the osteotomy plane was 45° relative to the posterior condylar axis of the tibia. Both the proximal and distal cuts of the osteotomy were slopped. A 10 mm medialization was performed. The model was fixed using 4.5 mm screws manufactured of Ti–6Al–4 V (Ti G5) alloy (Fig. 2a). There was no gap between the fragments at the osteotomy plane. For the fixation of the Fulkerson osteotomy, two parallel 4.5 mm cortical screws inserted in the sagittal plane toward the posterior tibial cortex are commonly recommended [6]. But, in line with the hypothesis in the current study (to stay away from the posterior neurovascular structures, to achieve a bicortical fixation, to capture the thicker posteromedial cortex of the tibia, and, most importantly, to achieve a fixation perpendicular to the osteotomy plane) the configuration of the screws was shifted toward the posteromedial cortex of the tibia in the axial plane. We also hypothesized that divergent screw placement might be more resistant to fragment sliding and gap formation. Thus, four different fixation scenarios were created on the basis of the above-mentioned principles (Fig. 2b).

Boundary conditions and material properties

Davis et al. [12] found that a TT osteotomy failure load fixed with two 4.5 mm cortical screws was 1654 N in a biomechanical study performed on fresh frozen cadavers.

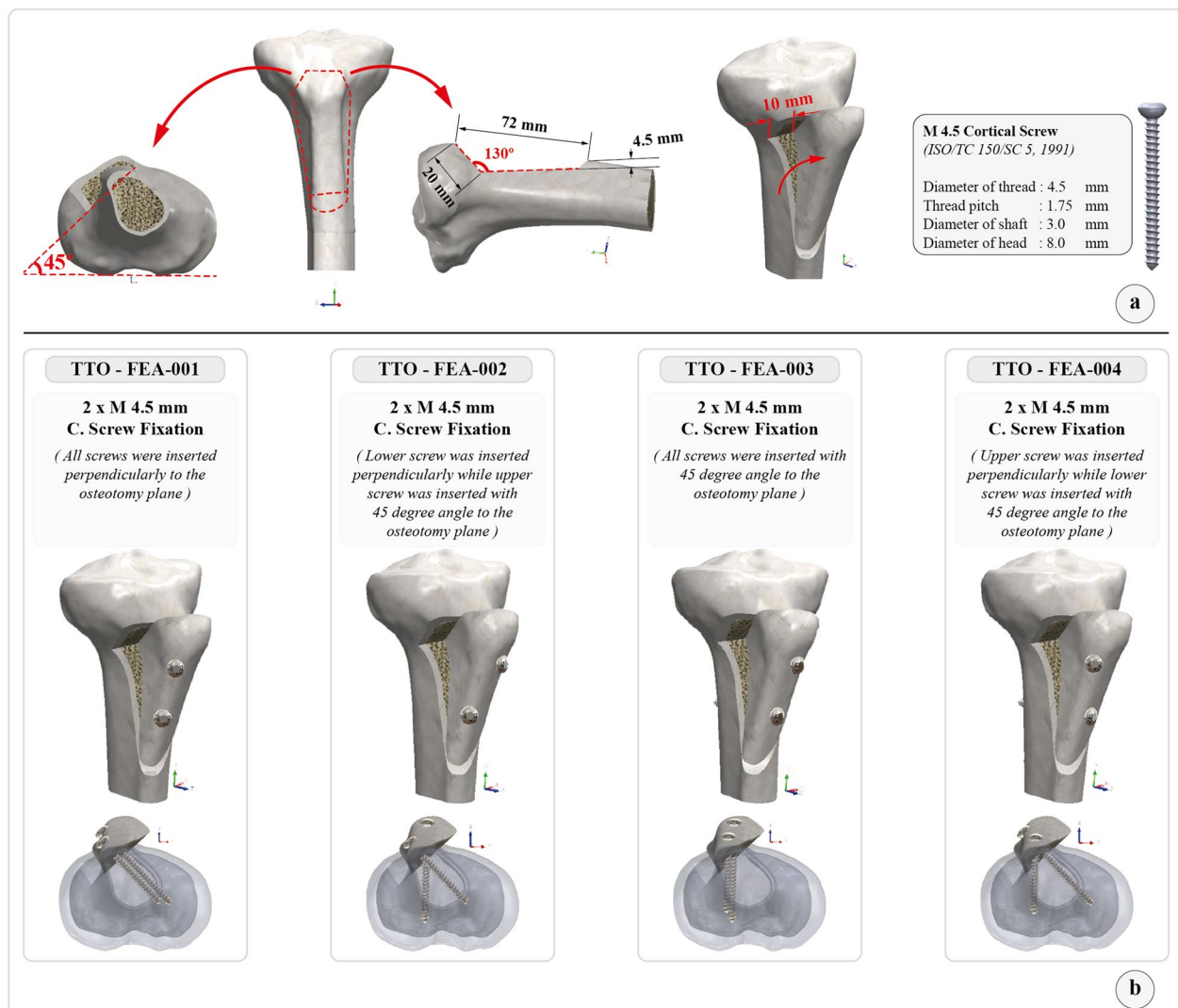


Fig. 2 **a** Solid model showing the details of Fulkerson osteotomy. The tibial tubercle fragment is 72 mm in length, the osteotomy plane is 45° to the posterior condylar axis, and 10 mm of medialization is performed. **(b)** The screw configurations and fixation scenarios tested in FEA

To simulate a worst-case scenario, a 1654 N traction force was applied to the patellar tendon footprint at the TT [12, 15, 16]. The total area of the patellar tendon footprint and the angle of the force vector was calculated from the CT data (Fig. 3). The tibia was fixed to the ground from its distal part in an anatomical position, and two supports at the medial and lateral condyles were placed on the proximal tibia. Frictional contact (nonlinear contact) between screw–bone surfaces and between bony fragment surfaces were defined in the 3D model. Furthermore, bonded contact definitions between cortical and trabecular bone were established. According to previous research, the screws were preloaded with 50 N, and the friction coefficients between bone-to-bone and

bone-to-screw were assigned 0.46 and 0.37, respectively [23–26]. Under the isotropic homogeneous linear elastic material model assumptions, material properties for cortical and trabecular bone and titanium alloy cortical screws were allocated independently (Table 2) [27–33].

Mesh structure and quality verification

The accuracy of FEA simulation is considerably affected by the quality of the mesh structure of a model. The skewness metric, which defines how near to ideal a face or cell is in a finite element model, is one of the key quality measurements for a mesh structure in an FEA. The skewness of a distribution may be used to determine its shape and asymmetry, allowing mesh structure

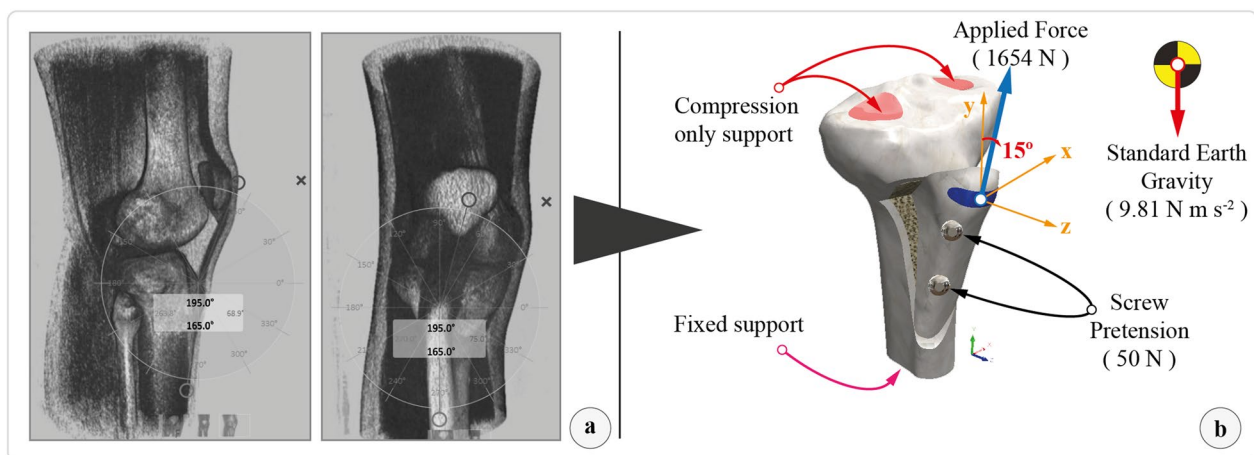


Fig. 3 **a** Volume-rendered 3D CT image from the lateral and anterior view. The patellar tendon footprint and the patellar tendon force vector were calculated. **b** Boundary condition of the models during loading

Table 2 Material properties assigned in the FEA set up in accordance with the homogeneous isotropic linear elastic material model

Material properties

Parameters	Unit	Model components		
		Cortical bone	Trabecular bone	Cortical screws (Ti-6Al-4 V)
Modulus of elasticity	(MPa)	19,100	1000.61	115,000
Poisson's ratio	(-)	0.30	0.30	0.33
Density	(kg m ⁻³)	1980	830	4500

FEA finite element analysis

verification [34]. A value of zero denotes an equilateral cell (best mesh quality), and a value of one indicates an utterly degenerate cell (worst mesh quality) according to the analysis code's definition of skewness [35]. As a result, the mesh structure in this study was verified using the skewness measure (mesh quality). The skewness values demonstrated high mesh quality for all of the cases evaluated, with a mean of 0.264 ± 0.01 . The final mesh structure of the solid models was created using a curvature-based meshing approach. An average of 1.38 million elements and 2.06 million nodes were found for all solid models. Figure 4 shows a visual representation of the meshing of the models. Each simulation scenario was run separately with identical boundary conditions after completing the preprocessor steps, and then visual and numerical outputs were recorded. A Dell Precision M4800 Series mobile workstation (Intel Core™ i7 4910MQ CPU @ 2.90 GHz, NVIDIA Quadro K2100M-2 GB, and Physical Memory: 32 GB) was used to solve the problem.

Assessment of sliding and separation

The magnitude of maximum gap formation and sliding distance between the osteotomy fragment and the tibia were calculated (Fig. 5). In addition, the equivalent (von Mises) stress and total deformation distributions on the components were retrieved from the simulation results.

Results

After loading the models with 1654 N patellar tendon traction force, the osteotomy fragment moved superiorly. Since the proximal cut is sloped (bevel-cut osteotomy), the osteotomy fragment slid and rested on the upper tibial surface. Afterward, the upper surface of the osteotomy fragment acted as a fulcrum, and the distal part of the fragment began to separate from the tibia while the screws resisted the displacement.

The average sliding through the upper and lower contact surfaces was the least in the fourth scenario (FEA-001: 0.165 mm, FEA-002: 0.182 mm, FEA-003: 0.133 mm, and FEA-004: 0.128 mm, respectively). The average gap

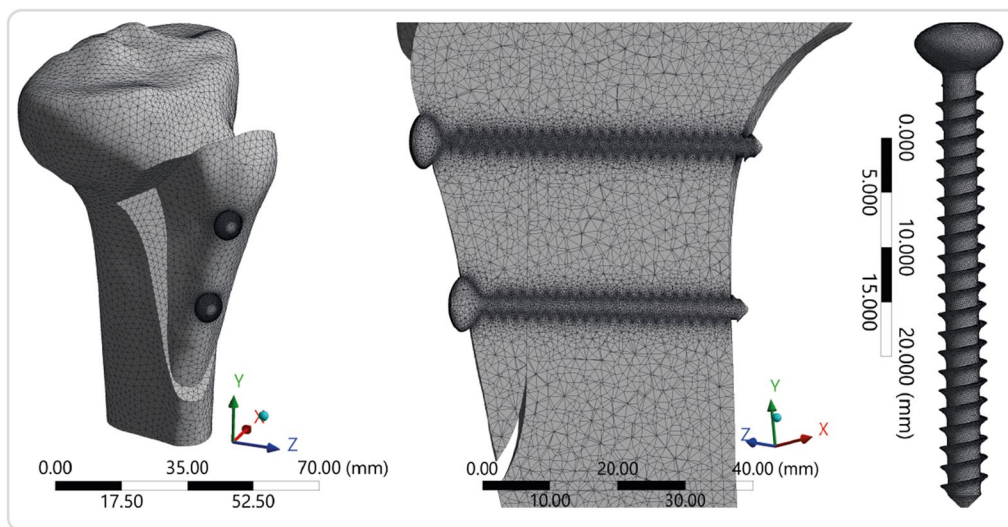


Fig. 4 The mesh structure of the model and screws

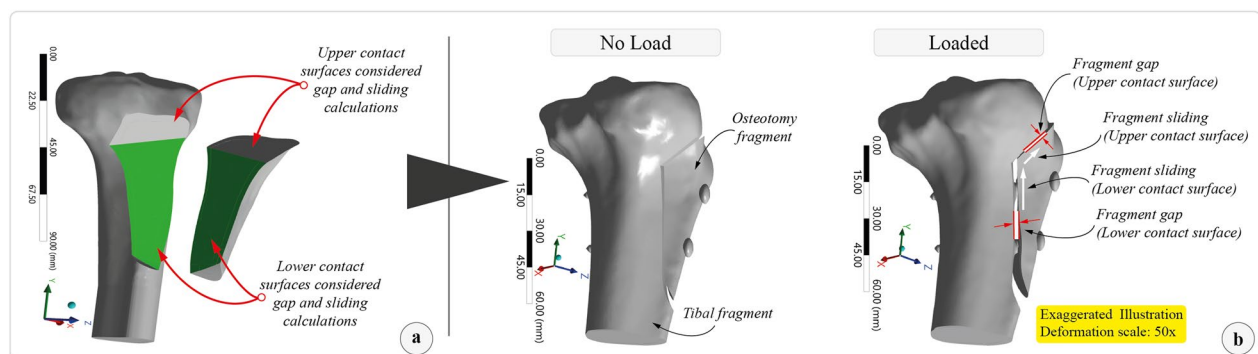


Fig. 5 **a** The contact surfaces of the osteotomy (upper and lower surface). **b** The sliding and gap formation was measured after loading independently

formation at the upper and lower contact surfaces was the least in the third scenario (FEA-001: 1.052 mm, FEA-002: 1.013 mm, FEA-003: 0.996 mm, and FEA-004: 1.025 mm, respectively). The resultant total displacement was the least in the fourth scenario (FEA-001: 0.319 mm, FEA-002: 0.307 mm, FEA-003: 0.333 mm, and FEA-004: 0.245 mm, respectively). Maximum frictional stress and maximum pressure between components on both surfaces were highest in the first scenario (FEA-001). The summary of the results is presented in Table 3.

Under predefined loading conditions, no permanent deformation or damage was detected on the screws. However, maximum equivalent (von Mises) stress values on the cortical and trabecular bone around the screw threads and the upper surface fulcrum point locally exceeded their yield stress points reported in previous studies [28, 32, 36, 37]. Figure 6 displays the visual simulation results for each scenario.

Discussion

The fourth model (FEA-004) demonstrated the least magnitude of sliding distance in the upper surface of the osteotomy as well as the least magnitude of maximum displacement. Therefore, the fourth model emerged as the most favorable screw configuration, with the highest stiffness among these models. Based on the findings of the current study, a divergent screw fixation in which the upper screw is inserted perpendicular to the osteotomy plane and the lower screw is inserted perpendicular to the posterior tibial cortex might be recommended.

The screw configuration proposed in this study has some advantages besides providing better stability. Two previous radiologic studies investigated the safe zone for TTO fixation to prevent iatrogenic popliteal vessel injury, a devastating complication of this procedure [8, 9]. The authors recommended routing the drill and screws toward the posteromedial cortex, which is safe

Table 3 The results of four models analyzed in terms of sliding distance, gap formation, resultant displacement, frictional stress, and pressure

FEA output	TTO—FEA-001		TTO—FEA-002		TTO—FEA-003		TTO—FEA-004	
	Upper surface	Lower surface	Upper surface	Lower surface	Upper surface	Lower surface	Upper surface	Lower surface
Maximum sliding distance	0.093	0.237	0.124	0.241	0.162	0.104	0.084	0.173
Average sliding	0.165		0.182		0.133		0.128	
Maximum gap	1.491	0.613	1.470	0.557	1.476	0.516	1.481	0.572
Average gap	1.052		1.013		0.996		1.025	
Maximum resultant displacement (entire model)	0.319		0.307		0.333		0.245	
Stiffness of the entire model	5185		5387		4967		6751	
Maximum frictional stress	25.094	3.802	23.285	3.307	19.287	2.888	21.158	3.255
Maximum pressure	54.552	8.264	50.619	7.188	41.928	6.279	45.996	7.076

FEA finite element analysis, TTO tibia tubercle osteotomy

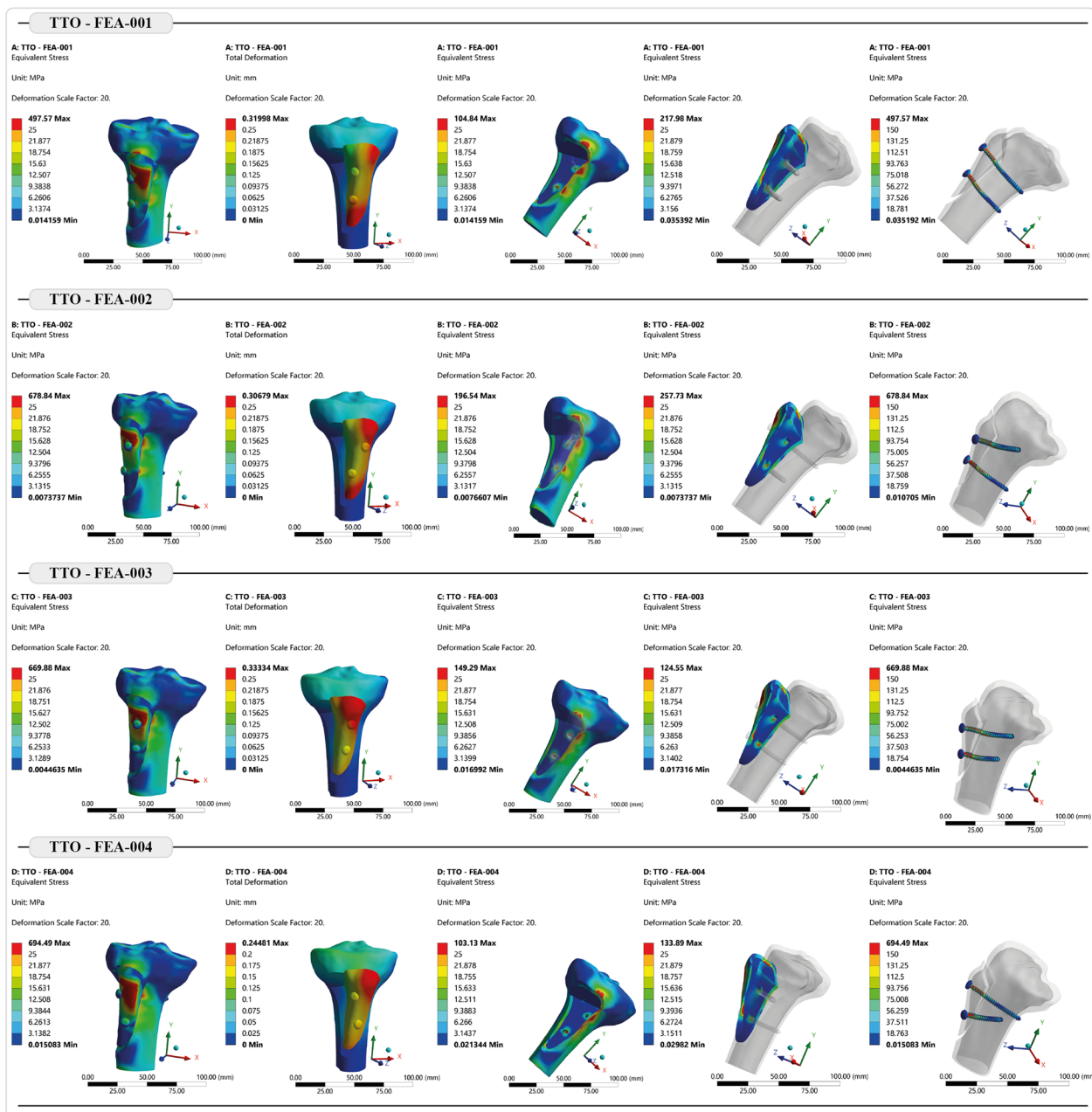


Fig. 6 Detailed visual simulation outputs of all tested scenarios

for bicortical fixation. In addition to being a safe zone for screw tips, the posteromedial cortex involves dense bone that provides better screw purchase. However, this analysis could not demonstrate the greatest results for the first model comprising two parallel screws perpendicular to the osteotomy plane. On the other hand, the popliteal artery gives its major peripheric branches approximately 5 cm distal to the tibial joint line. Thus, the risk of injury is higher in the upper screw than in the lower screw [38].

The divergent screw configuration proposed in this study might also significantly reduce the risk of vascular injury without impairing stability.

Secondly, this screw configuration might reduce the number of implant removal operations. The tibial tubercle is in contact with various surfaces during kneeling. Due to its prominence and relatively thin overlying soft tissue, the skin over the tibial tubercle area is vulnerable to irritation. Moreover, prominent hardware causes

significant discomfort. Therefore, hardware removal is the most frequent secondary surgical intervention performed following Fulkerson osteotomy [5]. A previous systematic review including 1055 TTO procedures reported an overall incidence of 19% hardware removal [39]. In another systematic review, 49% of the cases had undergone implant removal following Fulkerson osteotomy [3]. Moreover, some authors have recommended routine removal of the hardware after the union of TTO, regardless of the presence and severity of the symptoms [40, 41]. Since screw placement perpendicular to Fulkerson osteotomy allows better positioning of the screw head, deep to the tibialis anterior muscle belly, as shown in Fig. 1, this configuration seems more feasible to overcome the potential skin irritation. The findings of this study also favor the perpendicular insertion of the upper screw for better stability. Screws inserted perpendicular to the osteotomy plane from lateral to medial direction do not adversely affect the stability. The screw heads move away from the anterior direct contact surface and are covered by the muscle mass.

The majority of previous biomechanical studies have assessed the fixation techniques of TTO used in the extended exposure of revision knee arthroplasty [6, 11–19, 42]. Only a few studies have focused on the biomechanical features of flat and oblique TTO used to treat PF instability. These two osteotomies are technically different from each other. While medial displacement is not performed in TT osteotomy used in revision knee arthroplasty, medialization is performed in PF instability surgery. Secondly, the plane of osteotomy is oblique. Therefore, although these two osteotomies are similar in three-dimensional shape, the contact surface area decreases in medialization, and the patellar tendon loading condition is changed, so both osteotomies should be evaluated differently.

Cosgarea et al. [11] compared the fixation strengths of two 3.5 mm bicortical screws in flat and oblique TTOs in cadaveric tibiae. The authors reported superior results for flat osteotomy, despite a greater contact area in the oblique osteotomy line. However, flat osteotomies, also known as Elmslie–Trillat, are no longer preferred because they increase patellofemoral contact pressures and cause osteoarthritis in the long term. Another cadaveric study, conducted by Warner et al. [6], compared two 4.5 mm and three 3.5 mm cortical screws in Fulkerson osteotomy. Their results indicated more robust stability in two 4.5 mm screw fixations than in three 3.5 mm screw fixations. Using a cadaver model, Nurmi et al. [14] compared the bioabsorbable 4.5 mm poly-L-lactide (PLLA) screws with stainless-steel screws in the flat osteotomy. Although the stainless-steel screws demonstrated approximately two-fold higher stiffness, the

authors reported that the PLLA screws could resist the tractive forces of active knee extension. Furthermore, Ünal et al. [43] have reported favorable clinical outcomes in ten patients who had undergone Fulkerson osteotomy fixed with 4.8-mm headless bioabsorbable screws made of magnesium. Therefore, using bioabsorbable screws in the fixation of TTO seems practicable since it may avoid secondary procedures due to common hardware-related skin irritation.

Three previous FEA studies investigated the fixation of TTO used in the extended exposure of knee arthroplasty without medialization [15–17]. The first study assessed the fixation of flat tubercle osteotomy with two 4.5 mm titanium screws implanted in the configurations as follows: parallel horizontal, parallel downward, parallel upward, trapezoid, and divergent [16]. The authors reported the highest stability for parallel downward screw configuration depending on the least magnitude of fragment displacement and gap formation. The second study assessed three configurations of flat tubercle osteotomy (step cut, bevel cut, and straight cut) and various fixation configurations with two 4.5 mm screws [15]. Step cut was reported to be the most stable osteotomy configuration, based on the buttressing effect inherent in the step-cut technique. The third FEA study investigated the effect of gap formation between the distal and proximal sides of the tibial tubercle fragment on the stability of the fixation with different screw configurations [17]. The proximal gap model resulted in inferior results compared to the distal gap model in all screw configurations. Among the screw configurations, two parallel downward screws resulted in the highest stability in both models. Since the effect of tubercle medialization or anteromedialization has not been studied in the studies mentioned above [15–17], the present study is more predictive for TTO used to treat PF instability. Unlike these two studies, including the screw configurations with alterations in the sagittal plane, the present research biomechanically compared the screw configurations with modifications in the axial plane to avoid prominent hardware as much as possible.

Patellar height can be normalized by distalizing the TT during Fulkerson osteotomy in patients with accompanying patella alta. In the last FEA study, the biomechanical stability of the various 3.5 mm, 4.5 mm cortical screws and 3.5 mm 1/3 tubular plate-screw augmentation options were compared in Fulkerson osteotomy with distalization procedure [18]. Since the distal hinge and the proximal contact is lost in distalization procedures, the osteotomy becomes inherently unstable compared to a standard Fulkerson osteotomy. Thus, the authors recommended plate-screw-augmented fixation to achieve maximum stability. Although the osteotomy modeling differed from the current study, the screw configuration

was similar, and they advocated inserting the screws perpendicular to the osteotomy plane. All these previous FEA studies show that changing the screw configuration might increase the stability of the fixation construct in TT osteotomies.

The current study has various limitations as well as strengths. The inherent constraints of FEA must be considered while evaluating the results. Several preset assumptions were used, such as boundary conditions and material properties. Secondly, since the data in this FEA study are absolute values, a statistical comparison was not made. Despite the limitations of this study, it also has some strengths. CT data of a patient with patellofemoral instability and an increased TT–TG distance were employed to create a precise model to simulate the clinical reality. Since the bone is not uniform, the cortical and trabecular bones were separately defined with a bonded contact model. Although a cadaveric experiment did not validate the results of this FEA, it provides important information about the biomechanical characteristics of Fulkerson osteotomy and its fixation.

Conclusion

A divergent screw configuration in which the upper screw is inserted perpendicular to the osteotomy plane and the lower screw inserted perpendicular to the posterior tibial cortex (FEA-004) might be a better option for the fixation of Fulkerson osteotomy. Surgeons who prefer two 4.5 mm cortical screws for Fulkerson osteotomy fixation can achieve a more stable fixation by applying this simple modification in screw configuration. In addition, this modification may reduce the risk of neurovascular injuries and thus allow safer bicortical screw fixation. Finally, it can reduce the need for implant removal by shifting the screw heads away from the direct contact area of the knee. However, these propositions need to be supported by further clinical studies.

Abbreviations

AO	Arbeitsgemeinschaft für Osteosynthesefragen
CT	Computerized tomography
FEA	Finite element analysis
PF	Patellofemoral
Ti	Titanium
TT	Tibial tubercle
TTO	Tibial tubercle osteotomy
TT–TG	Tibial tubercle–trochlear groove
Q angle	Quadriceps angle
3D	Three-dimensional

Acknowledgements

Not applicable

Author contributions

Study conception and design: FA, OK, HKC, MEU Acquisition of data: OK, HKC, FA, ET, BG Analysis and interpretation of data: OK, AC, ET, HKC, Drafting of the

manuscript: BG, OK, HKC, ET, AC, MEU, Critical revision: FA, OK, AC, ET, HKC, BG, MEU.

Funding

No funds have been received for this study.

Availability of data and materials

The datasets generated during and/or analyzed during the current study are available from the corresponding author upon reasonable request.

Declarations

Ethics approval and consent to participate

Formal ethics approval was waived for this virtual computer-based analysis.

Consent for publication

Written informed consent was obtained from the patient to the anonymous use of the imaging files.

Competing interests

The authors declare that they have no competing interests.

Author details

¹Vocational School of Health Services, SANKO University, Gaziantep, Turkey. ²Department of Orthopedics and Traumatology, Antalya Training and Research Hospital, Varlık mah., Kazım Karabekir cd., Muratpasa, 07100 Antalya, Turkey. ³Department of Orthopedics and Traumatology, Adana City Education and Research Hospital, Adana, Turkey. ⁴Agricultural Faculty, Department of Agricultural Machinery and Technology Engineering, Akdeniz University, Antalya, Turkey. ⁵Department of Orthopedics and Traumatology, Istanbul Training and Research Hospital, Istanbul, Turkey. ⁶Department of Orthopedics and Traumatology, Prof. Dr. Cemil Tascioglu City Hospital, Istanbul, Turkey. ⁷Department of Manufacturing, Polytechnic University of Bucharest, Bucharest, Romania.

Received: 23 September 2022 Accepted: 4 June 2023

Published online: 26 June 2023

References

- Maffulli N (2018) Editorial commentary: standing the test of time and sport: Fulkerson tibial tubercle osteotomy of the knee. *Arthroscopy* 34(4):1030–1031. <https://doi.org/10.1016/j.arthro.2017.12.023>
- Noyes FR, Barber-Westin SD (2017) Operative Options for Extensor Mechanism Malalignment and Patellar Dislocation. In: Noyes FR (ed) *Noyes' Knee Disorders: Surgery, Rehabilitation, Clinical Outcomes*, 2nd edn. Elsevier, Philadelphia
- Payne J, Rimmke N, Schmitt LC, Flanigan DC, Magnussen RA (2015) The incidence of complications of tibial tubercle osteotomy: a systematic review. *Arthroscopy* 31(9):1819–1825. <https://doi.org/10.1016/j.arthro.2015.03.028>
- Knapik DM, Kunze KN, Azua E, Vadhera A, Yanke AB, Chahla J (2021) Radiographic and clinical outcomes after tibial tubercle osteotomy for the treatment of patella alta: a systematic review and meta-analysis. *Am J Sports Med* 26:3635465211012371. <https://doi.org/10.1177/03635465211012371>
- Johnson AA, Cosgarea AJ, Wolfe EL (2017) Complications of tibial tuberosity osteotomy. *Sports Med Arthrosc Rev* 25(2):85–91. <https://doi.org/10.1097/JSA.0000000000000151>
- Warner BT, Kamath GV, Spang JT, Weinhold PS, Creighton RA (2013) Comparison of fixation methods after anteromedialization osteotomy of the tibial tubercle for patellar instability. *Arthroscopy* 29(10):1628–1634. <https://doi.org/10.1016/j.arthro.2013.06.020>
- Taha W (2018) Screws. In: Buckley RE, Apivatthakakul T (eds) *AO principles of fracture management*, 3rd edn. Thieme, New York
- Hernigou J, Chahidi E, Kashi M, Moest E, Dakhil B, Hayek G et al (2018) Risk of vascular injury when screw drilling for tibial tuberosity transfer. *Int Orthop* 42(5):1165–1174. <https://doi.org/10.1007/s00264-017-3554-7>

9. Shetty AA, Tindall AJ, Nickolaou N, James KD, Ignotus P (2005) A safe zone for the passage of screws through the posterior tibial cortex in tibial tubercle transfer. *Knee* 12(2):99–101. <https://doi.org/10.1016/j.knee.2004.03.010>
10. Fulkerson JP (1983) Anteromedialization of the tibial tuberosity for patellofemoral malalignment. *Clin Orthop Relat Res* 177:176–181
11. Cosgarea AJ, Schatzke MD, Seth AK, Litsky AS (1999) Biomechanical analysis of flat and oblique tibial tubercle osteotomy for recurrent patellar instability. *Am J Sports Med* 27(4):507–512. <https://doi.org/10.1177/03635465990270041601>
12. Davis K, Caldwell P, Wayne J, Jiranek WA (2000) Mechanical comparison of fixation techniques for the tibial tubercle osteotomy. *Clin Orthop Relat Res* 380:241–249. <https://doi.org/10.1097/00003086-200011000-00033>
13. Caldwell PE, Bohlen BA, Owen JR, Brown MH, Harris B, Wayne JS et al (2004) Dynamic confirmation of fixation techniques of the tibial tubercle osteotomy. *Clin Orthop Relat Res* 424:173–179. <https://doi.org/10.1097/01.blo.0000130205.57095.a2>
14. Nurmi JT, Itälä A, Sihvonen R, Sillanpää P, Kannus P, Sievänen H et al (2017) Bioabsorbable versus metal screw in the fixation of tibial tubercle transfer: a cadaveric biomechanical study. *Orthop J Sports Med* 5(7):2325967117714433. <https://doi.org/10.1177/2325967117714433>
15. Chang CW, Chen YN, Li CT, Chung CR, Chang CH, Peng YT (2019) Finite element study of the effects of fragment shape and screw configuration on the mechanical behavior of tibial tubercle osteotomy. *J Orthop Surg (Hong Kong)* 27(3):2309499019861145. <https://doi.org/10.1177/2309499019861145>
16. Chang CW, Chen YN, Li CT, Chung CR, Tseng CC, Chang CH, Peng YT (2019) Biomechanical investigation of tibial tubercle osteotomy fixed with various screw configurations. *Injury* 50(2):263–271. <https://doi.org/10.1016/j.injury.2018.12.004>
17. Chen Y, Li CT, Peng YT (2019) Gap between the fragment and the tibia affects the stability of tibial tubercle osteotomy: a finite element study. *Med Eng Phys* 68:57–64. <https://doi.org/10.1016/j.medengphy.2019.03.012>
18. Guneri B, Kose O, Celik HK, Cakar A, Tasatan E, Rennie AEW (2022) How to fix a tibial tubercle osteotomy with distalisation: a finite element analysis. *Knee* 37:132–142. <https://doi.org/10.1016/j.knee.2022.06.002>
19. Frame M, Hauck O, Newman M, Cirtautas A, Wijdicks C (2021) Suture tape augmentation of screw fixation reduces fragment migration in tibial tubercle osteotomy: a biomechanical study. *Orthop J Sports Med* 9(10):23259671211038496. <https://doi.org/10.1177/23259671211038496>
20. Mehta S, Tyler A, Hast M (2017) Understanding the basics of computational models in orthopaedics: a nonnumeric review for surgeons. *J Am Acad Orthop Surg* 25(10):684–692. <https://doi.org/10.5435/JAAOS-D-16-00320>
21. Lewis GS, Mischler D, Wee H, Reid JS, Varga P (2021) Finite element analysis of fracture fixation. *Curr Osteoporos Rep* 19(4):403–416. <https://doi.org/10.1007/s11914-021-00690-y>
22. Heller MO (2022) Finite element analysis in orthopedic biomechanics. In: Innocenti B, Galbusera F (eds) *Human orthopaedic biomechanics*. Academic Press, New York
23. Celik T (2021) Biomechanical evaluation of the screw preload values used in the plate placement for bone fractures. *Proc Inst Mech Eng [H]* 235(2):141–147. <https://doi.org/10.1177/0954411920964628>
24. Eberle S, Gerber C, von Oldenburg G, Högel F, Augat P (2010) A biomechanical evaluation of orthopaedic implants for hip fractures by finite element analysis and in-vitro tests. *Proc Inst Mech Eng H* 224(10):1141–1152. <https://doi.org/10.1243/09544119JHEIM799>
25. Gao X, Fraulob M, Haiat G (2019) Biomechanical behaviours of the bone-implant interface: a review. *J R Soc Interface* 16(156):20190259. <https://doi.org/10.1098/rsif.2019.0259>
26. Hayes WC, Perren SM (1972) Plate–bone friction in the compression fixation of fractures. *Clin Orthop Relat Res* 89:236–240
27. Alonso-Rasgado T, Jimenez-Cruz D, Karski M (2017) 3-D computer modeling of malunited posterior malleolar fractures: effect of fragment size and offset on ankle stability, contact pressure and pattern. *J Foot Ankle Res* 10:13. <https://doi.org/10.1186/s13047-017-0194-5>
28. Dong XN, Acuna RL, Luo Q, Wang X (2012) Orientation dependence of progressive post-yield behaviour of human cortical bone in compression. *J Biomech* 45(16):2829–2834. <https://doi.org/10.1016/j.jbiomech.2012.08.034>
29. Kim SH, Chang SH, Jung HJ (2010) The finite element analysis of a fractured tibia applied by composite bone plates considering contact conditions and time-varying properties of curing tissues. *Compos Struct* 92:2109–2118. <https://doi.org/10.1016/j.compstruct.2009.09.051>
30. Klekiel T, Będziński R (2015) Finite element analysis of large deformation of articular cartilage in upper ankle joint of occupant in military vehicles during explosion. *Arch Metall Mater* 60:2115–2121. <https://doi.org/10.1515/amm-2015-0356>
31. Novitskaya E, Zin C, Chang N, Cory E, Chen P, D'Lima D et al (2014) Creep of trabecular bone from the human proximal tibia. *Mater Sci Eng C Mater Biol Appl* 40:219–227. <https://doi.org/10.1016/j.msec.2014.03.057>
32. Oldani C, Dominguez A (2012) Titanium as a biomaterial for implants in recent advances in arthroplasty. InTech. <http://www.intechopen.com/books/recent-advances-in-arthroplasty/titanium-as-a-biomaterial-for-implants>. Accessed 30 Nov 2021
33. Wang X, Nyman JS, Dong X, Leng H, Reyes M (2010) Fundamental biomechanics in bone tissue engineering. *Synthesis Lectures Tissue Eng* 2(1):1–225. <https://doi.org/10.2200/s00246ed1v01y200912tis004>
34. Brys G, Hubert M, Struyf A (2004) A robust measure of skewness. *J Comput Graph Stat* 13(4):996–1017. <https://doi.org/10.1198/106186004X12632>
35. ANSYS Product Doc. ANSYS Meshing User's Guide: Skewness (Release 2019 R2). ANSYS Inc, USA. https://ansyshelp.ansys.com/account/secured?returnurl=/Views/Secured/corp/v191/wb2_help/wb2_help.html. Accessed 25 Sep 2020.
36. Jensen NC, Hvid I, Krøner K (1988) Strength pattern of cancellous bone at the ankle joint. *Eng Med* 17(2):71–76. https://doi.org/10.1243/emed_jour_1988_017_020_02
37. Sierpowska J, Hakulinen MA, Töyräs J, Day JS, Weinans H, Jurvelin JS et al (2005) Prediction of mechanical properties of human trabecular bone by electrical measurements. *Physiol Meas* 26(2):S119–S131. <https://doi.org/10.1088/0967-3334/26/2/012>
38. May H, Kastan O, Emre TY, Cetin M, Unal M, Kose O (2022) Anterior tibial artery and its clinical importance in the posterolateral approach to the tibial plateau: an angiographic study on 219 lower limbs. *J Knee Surg* 35(7):725–730. <https://doi.org/10.1055/s-0040-1716849>
39. Saltzman BM, Rao A, Erickson BJ, Cvetanovich GL, Levy D, Bach BR Jr et al (2017) A systematic review of 21 tibial tubercle osteotomy studies and more than 1000 knees: indications, clinical outcomes, complications, and reoperations. *Am J Orthop (Belle Mead NJ)* 46(6):E396–E407
40. Shelbourne KD, Porter DA, Rozzi W (1994) Use of a modified Elmslie–Trillat procedure to improve abnormal patellar congruence angle. *Am J Sports Med* 22:318–323. <https://doi.org/10.1177/036354659402200304>
41. Tecklenburg K, Feller JA, Whitehead TS, Webster KE, Elzarka A (2010) Outcome of surgery for recurrent patellar dislocation based on the distance of the tibial tuberosity to the trochlear groove. *J Bone Joint Surg Br* 92(10):1376–1380. <https://doi.org/10.1302/0301-620X.92B10.24439>
42. Chalidis B, Kitridis D, Givissis P (2020) Tibial tubercle osteotomy in revision total knee arthroplasty: a systematic review. *World J Orthop* 11(6):294–303. <https://doi.org/10.5312/wjo.v11.i6.294>
43. Ünal M, Demirayak E, Ertan MB, Kilicaslan OF, Kose O (2021) Bioabsorbable magnesium screw fixation for tibial tubercle osteotomy; a preliminary study. *Acta Biomed*. 92(6). <https://mattioli1885journals.com/index.php/actabiomedica/article/view/11716>. Accessed 27 Nov 2021.

Publisher's Note

Springer Nature remains neutral with regard to jurisdictional claims in published maps and institutional affiliations.